J Appl Electrochem (2013) 43:735–748
DOI 10.1007/s10800-013-0564-z

ORIGINAL PAPER

A new method for grafting functional groups onto mesoporous silica: an electrochemical approach

Mostafa M. Amini · Hamid Reza Lotfi Zadeh Zhad · Omid Sadeghi · Mohammad Hossein Banitaba · Saied Saeed Hosseiny Davarani

Received: 13 March 2013 / Accepted: 9 May 2013 / Published online: 18 May 2013

Abstract A novel method for the modification of mesoporous silica, MCM-41, using an electrochemical approach has been developed, and the process was monitored by cyclic voltammetery and spectrometric methods. The method was applied to the modification of mesoporous silica with new functional groups which are not accessible by conventional methods. Malononitrile-functionalized MCM-41 mesoporous silica was characterized by low-angle X-ray diffraction, Fourier transform infrared spectroscopy, mass spectrometry, thermal analysis, elemental analysis, high resolution transmission electron microscopy, and surface area measurement (S_{BET}). In addition, the application of malononitrile-functionalized MCM-41 as a sorbent for gold ions was demonstrated.

Keywords Nanostructure · Chemical synthesis · Electrochemical functionalization · Surface properties · Mesoporous silica

1 Introduction

After discovery of the mesoporous silica in 1992 by the Mobil Corporation, significant attention has been attracted to the utilization of these materials in various fields. In spite of the high thermal and mechanical stability [1] of mesoporous silica, their application in the absence of surface modifications and functionalization is limited. The traditional applications of these materials were limited their usage as catalysts [2] and adsorbents [3]. Recently, by the aid of modification of these materials, new applications such as medical diagnostics [4], microelectronics [5], optics [6], sensing materials [7, 8], and drug delivery [9] are reported for them. Therefore, during the past decade, numerous functional groups have been introduced onto the surface of mesoporous silica by various methods and with the introduction of each new functional group, a new application can be explored [10, 11]. Although, due to the low reactivity of the modifiers, the number of functional groups that can be introduced onto the surface of mesoporous silica is limited [12]. Therefore, developing an alternative method for silica functionalization will expand the application range of these materials.

The electrochemical synthesis of organic compounds is a well-established technique and has been widely implemented for the synthesis of materials that are not accessible by conventional methods [13]. Electrochemical syntheses of organic compounds are green methods that utilize environmentally friendly solvents, which is a great advantage of these methods [14]. In addition, it is possible to monitor the synthesis process by electrochemical methods [15]. In spite of the vast contribution of these methods to all areas of chemical technology, they have not been utilized for the anchoring of organic species onto mesoporous materials. In this work, an electrochemical synthesis method was implemented for the first time as a novel and powerful method for the functionalization of mesoporous silica with a new functional group, a process that is not accessible by other methods. In contrast to the conventional chemical methods for modification of mesoporous silica, no catalysts and/or heating was used for the modification progress. Furthermore, the method was

M. M. Amini · M. H. Banitaba · S. S. H. Davarani (✉)
Department of Chemistry, Shahid Beheshti University, G.C., 1983963113 Tehran, Iran
e-mail: sshosseiny@sbu.ac.ir

H. R. L. Z. Zhad · O. Sadeghi
Department of Chemistry, Shahr-e-Rey Branch, Islamic Azad University, P.O. Box 18735-334, Tehran, Iran

performed in a green solvent. This method opens up a new path for functionalization of mesoporous silica.

2 Experimental

2.1 Chemicals

Analytical grade reagents were purchased from E-Merck Company (Darmstadt, Germany) or from Fluka Company (Buchs SG, Switzerland) and used without further purification. *MCM-41* (**1**) mesoporous silica was prepared according to the reported procedure [16]. Synthesis of mesoporous silica was confirmed by IR spectroscopy and low-angle X-ray powder diffraction. *Amine-functionalized MCM-41* (**3**) was prepared by reacting *MCM-41* (**1**) with 3-*aminopropyltriethoxysilane* [$(C_2H_5O)_3SiCH_2CH_2CH_2$–$NH_2$ (**2**)], with the general procedure used to prepare amine-functionalization silica [17]. The formation of *amine-functionalized MCM-41* (**3**) was confirmed by IR spectroscopy and elemental analysis.

2.2 Apparatus

Cyclic voltammetry (CV) and preparative steps were performed using μ-Autolab potentiostat/galvanostat type III. A glassy carbon disc (1.8 mm diameter, 2.5 mm^2 area) was used as the working electrode (WE) in the voltammetry experiment and a platinum wire as the counter electrode (CE). Prior to each voltammetric measurement, the solution was sonicated for 5 min. The WE used in electrolysis was an assembly of three carbon rods (8 mm diameter, 4 cm length, and 25 cm^2 area) and a large platinum gauze constituted the CE. The WE potentials were adjusted versus Ag/AgCl/KCl (3 M) as a reference electrode. The solution was stirred during the electrolysis in order to prevent the settling of MCM-41 silica particles. All electrochemical studies were performed in Na_2HPO_4/NaH_2PO_4 (0.2 M, pH 7.2) buffer solutions. All pH measurements were carried out at 25 ± 1 °C with a digital WTW Metrohm 827 Ion analyzer (Herisau, Switzerland) equipped with a combined glass-calomel electrode. Specific surface area was measured by the nitrogen adsorption technique using a Micromeritics ASAP 2010 analyzer. Thermal analysis (TGA–DTA) was performed on a Bahr STA-503 (GmbH, Germany) instrument under air atmosphere with a heating rate of 10 °C min^{-1}. The CHN analyses were carried out on a Thermo Finnigan Flash-1112EA microanalyzer (Italy). X-ray diffraction (XRD) patterns were obtained on a STOE diffractometer with Cu K_α radiation. IR spectra were recorded on a BOMEM/MB series spectrophotometer. Gold concentration was determined by an AA-680 Shimadzu (Kyoto, Japan) flame atomic absorption spectrometer (FAAS) in an air-acetylene flame, according to the user's manual, provided by the manufacturer. A gold hollow cathode lamp was used as the radiation source with a wavelength of 242.8 nm. High resolution transmission electron microscopy (HRTEM) was performed on a Philips CM200. The mass spectra were obtained using a QP-1100EX Shimadzu GC-MS (EI at 70 eV).

2.3 Preparation of *chemically catechol-modified MCM-41* (**5**)

The *amine-functionalized MCM-41* (**3**) was reacted with *3,4-dihydroxybenzaldehyde* (**4**) to prepare *chemically catechol-functionalized MCM-41* (**5**). In this approach, 1.0 g of *amine-functionalized MCM-41* (**3**) was suspended in a mixture of 50 mL toluene and 1.0 g of *3,4-dihydroxybenzaldehyde* (**4**) and the mixture was refluxed for 24 h. Then the brownish solid was separated by filtration and washed with ethanol.

2.4 Preparation of *electrochemically catechol-modified MCM-41* (**14**)

A galvanostatic electro-organic synthesis method was used to prepare *electrochemically catechol-modified MCM-41* (**14**). In this approach, an aqueous solution of 2 mmol L^{-1} of catechol (**12**) and 250 mg of *amine-functionalized MCM-41* (**3**) were electrolyzed at 5 mA in an undivided cell. After 48 h, the electrolysis was stopped, and the product [*electrochemically catechol-modified MCM-41* (**14**)], which under the electrolysis conditions was in equilibrium with *o-quinone-modified MCM-41* (**15**), was filtered and washed with water and ethanol.

2.5 Preparation of *malononitrile-functionalized MCM-41* (**10/11**) and/or (**16/17**) by electrochemical method

To synthesize *malononitrile-functionalized MCM-41 silica* [Schemes 1, (**10/11**) or 2, (**16/17**)] in two separate bulks, 250 mg of *chemically catechol-modified MCM-41* (**5**) or *electrochemically catechol-modified MCM-41* (**14**) and 25 mg of *malononitrile* (**8**) were suspended in 100 mL of Na_2HPO_4/NaH_2PO_4 buffer solution (0.2 M, pH 7.2). *Malononitrile* (**8**) is in an equilibrium with *malononitrile anion* (**9**) in phosphate buffer solution (0.2 M, pH 7.2). The mixtures were electrolyzed at 5 mA for 48 h and the final products were removed and washed with water and ethanol.

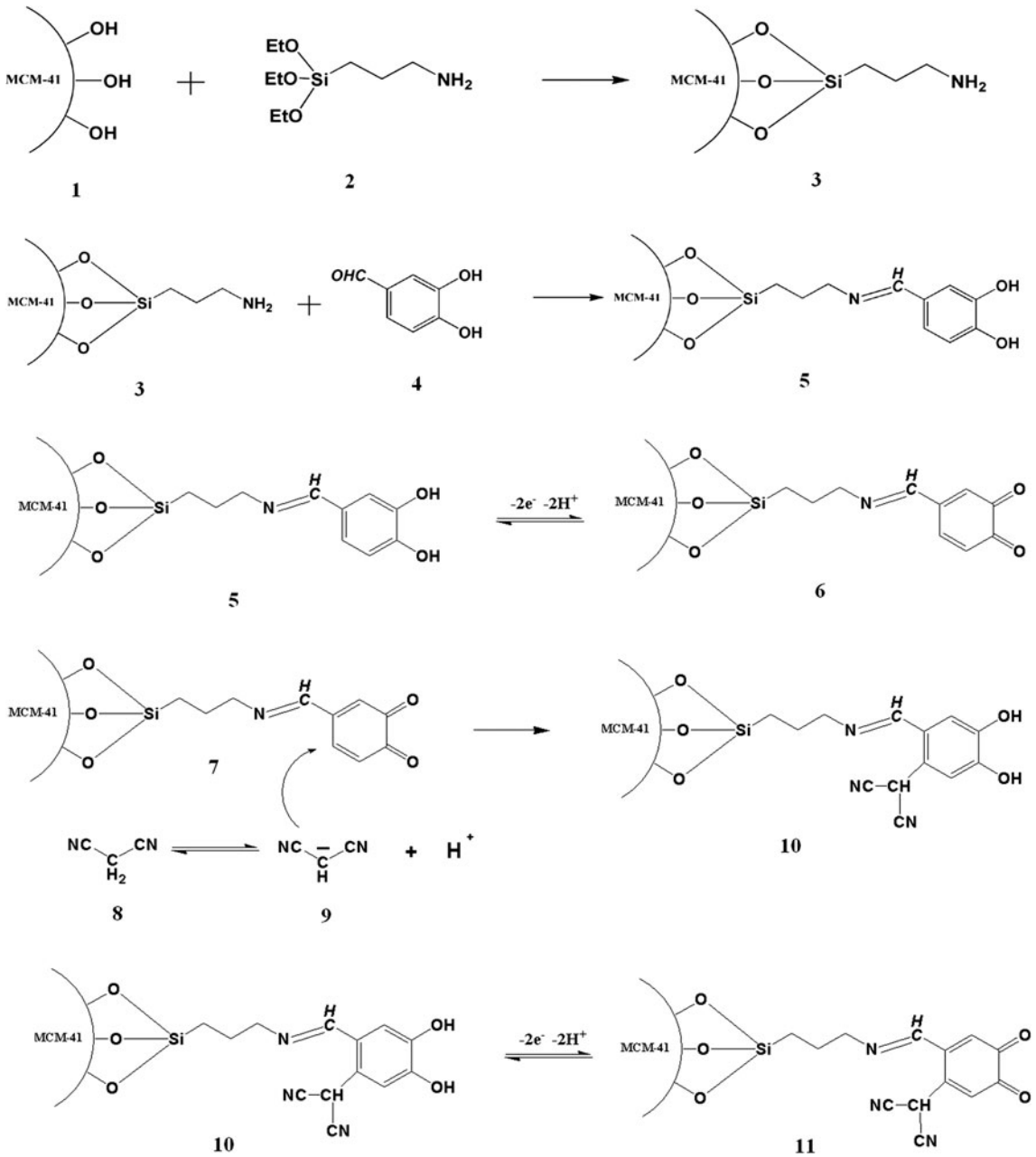

Scheme 1 A schematic diagram for synthesis of *chemically catechol-modified MCM-41* (**5**) and *malononitrile- functionalized MCM-41* (**10/11**)

3 Results and discussion

The electrochemical process was completely monitored. In the first step, the electrochemical reaction of *4-methylcatechol* (**18**) with *malononitrile* (**8**) was studied, and the electroreactivity of these compounds was observed. Then, *MCM-41* (**1**) was chemically modified with catechol, and the electroreactivity of this compound [*chemically catechol-functionalized MCM-41* (**5**)] with *malononitrile* (**8**) was studied. In the next section, *MCM-41* (**1**) was electrochemically modified with both catechol and *malononitrile* (**8**), and the electro-reactivity of *amine-functionalized MCM-41* (**3**) with *catechol* (**12**) was investigated.

3.1 Study the reactivity of catechol with *malononitrile* (**8**)

The electrochemical behavior of *4-methylcatechol* (**18**) in the presence and absence of *malononitrile* (**8**) as a nucleophile was studied using the CV method. The cyclic voltammogram of a solution containing 1 mmol L^{-1} of *4-methylcatechol*

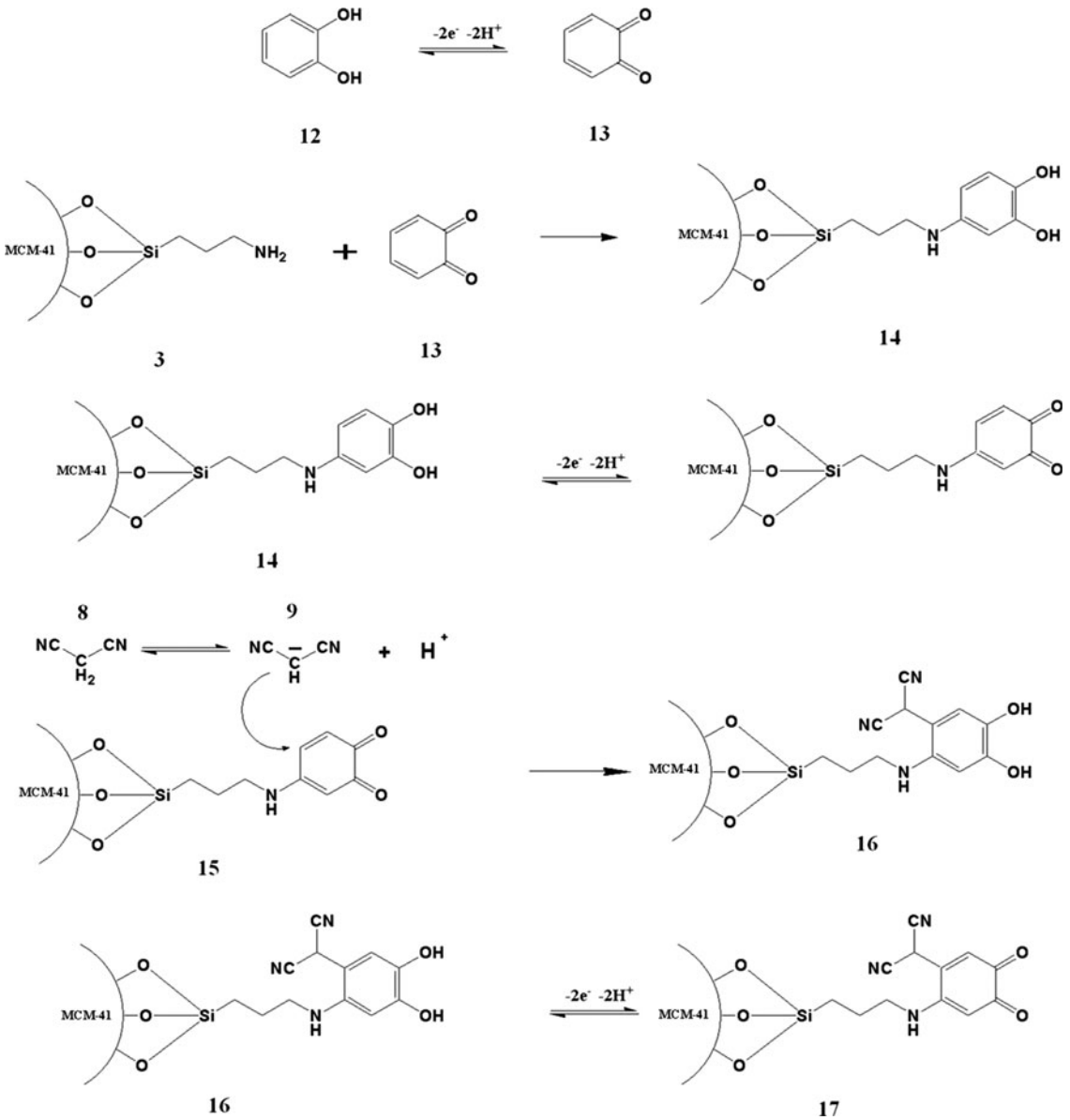

Scheme 2 A schematic diagram for synthesis of *electrochemically catechol-modified MCM-41* (**14**) and *malononitrile-functionalized MCM-41* (**16/17**)

(**18**) is shown in Fig. 1a, curve a (in Na_2HPO_4/NaH_2PO_4 (0.2 M, pH 7.2) buffer solution). The anodic peak A_1 and the corresponding cathodic peak C_1 appear due to the transformation of *4-methylcatechol* (**18**) to *4-methyl-o-quinone* (**19**), and vice versa, within a quasireversible two-electron/two-proton reaction. In this reaction, the peak current ratio $I_p^{C_1}/I_p^{A_1}$ is nearly equal to 1, which can be considered as a marker for the stability of *o*-benzoquinone produced at the surface of the electrode under the experimental conditions. In other words, any hydroxylation [18] or dimerization [19] reactions are too slow to be observed within the time scale of the CV. Figure 1a, curve b shows the cyclic voltammogram of a solution containing 1 mmol L^{-1} *4-methylcatechol* (**18**) and 1 mmol L^{-1} *malononitrile* (**8**) (in the same buffer solution). As a result of the reaction between *malononitrile* (**8**) and *4-methyl-o-quinone* (**19**), the cathodic peak current (C_1) disappeared in this voltammogram. The new cathodic peak (C_0) appeared in curve b is related to reduction of 2-*(6-methyl-3,4-dicyclohexa-1,5-dien-1-yl)malononitrile* (**21**) *to 2-(4,5-dihydroxy-2-methylphenyl)malononitrile* (**20**). The curve c is the voltammogram of a solution containing 1 mmol L^{-1} *malononitrile* (**8**) (in the same solution and under the same conditions).

The multicyclic voltammograms of a solution containing 1 mmol L^{-1} *4-methylcatechol* (**18**) in the presence of 1 mmol L^{-1} *malononitrile* (**8**) were studied, and are

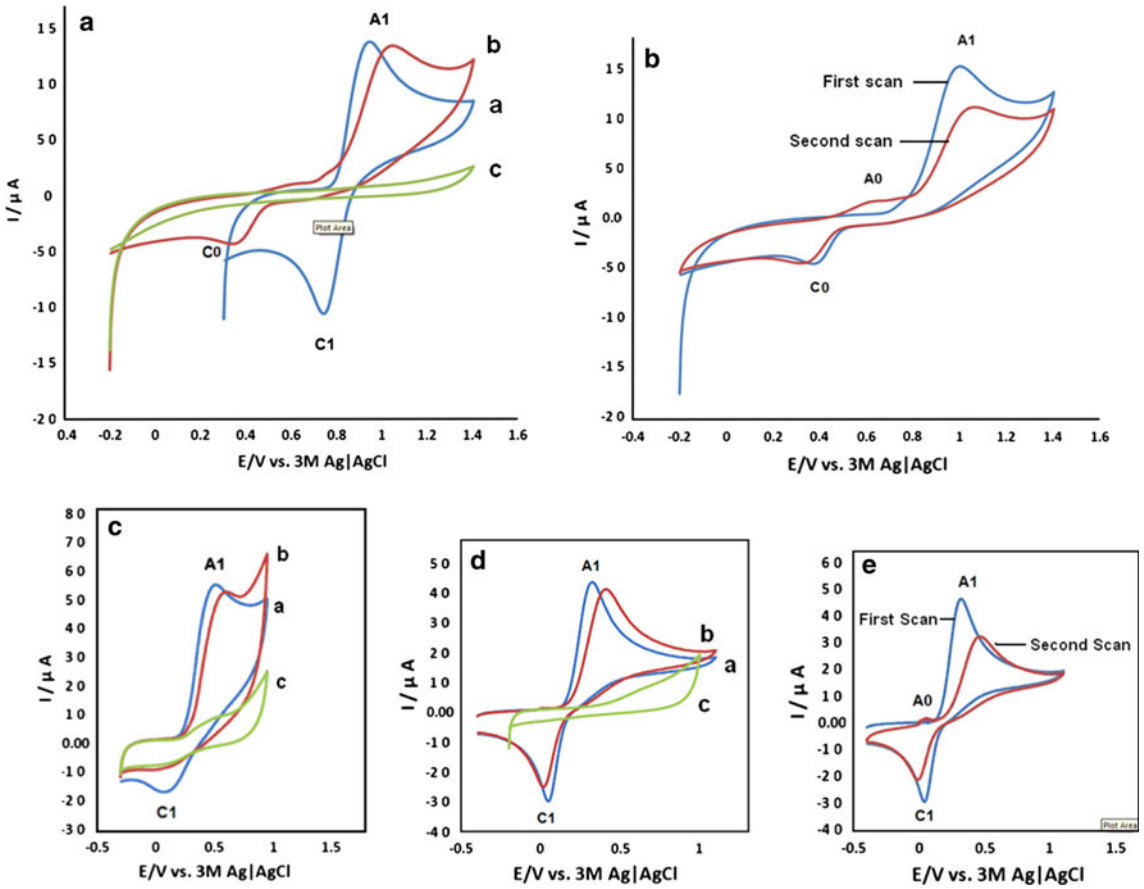

Fig. 1 **a** (*a*) Cyclic voltammograms of 1 mM *4-methylcatechol* (**18**), (*b*) cyclic voltammograms of 1 mM *4-methylcatechol* (**18**) in the presence of 1 mM *malononitrile* (**8**), (*c*) cyclic voltammograms of 1 mM *malononitrile* (**8**), scan rate = 100 mV s^{-1}; **b** multicyclic voltammograms of 1 mM *4-methylcatechol* (**18**) in the presence of 1 mM of *malononitrile* (**8**), scan rate = 100 mV s^{-1}; **c** (*a*) cyclic voltammograms of 250 mg *chemically catechol-modified MCM-41* (**5**), (*b*) cyclic voltammograms of 250 mg *chemically catechol-modified MCM-41* (**5**) in the presence 25 mg of *malononitrile* (**8**), (*c*) cyclic voltammograms of 25 mg *malononitrile* (**8**), scan rate = 500 mV s^{-1}; **d** (*a*) cyclic voltammograms of 2 mM *catechol* (**12**), (*b*) cyclic voltammograms of 2 mM *catechol* (**12**) in the presence of 0.25 g *amine-functionalized MCM-41* (**3**), (*c*) cyclic voltammograms of 0.25 g *amine-functionalized MCM-41* (**3**); **e** multicyclic voltammograms of 2 mM *catechol* (**12**) in the presence of 0.25 g *amine-functionalized MCM-41* (**3**), scan rate = 100 mV s^{-1}; All at a glassy carbon electrode in 100 mL phosphate buffer solution (pH 7.2, 0.2 M); room temperature

presented in Fig. 1b. In the second cycle, a new anodic peak, A_0, appeared. This new peak belongs to the oxidation of the intermediate *2-(4,5-dihydroxy-2-methylphenyl)malononitrile* (**20**) to *2-(6-methyl-3,4-dicyclohexa-1,5-dien-1-yl)malononitrile* (**21**). The cathodic peak (C_0) is related to reduction of *2-(6-methyl-3,4-dicyclohexa-1,5-dien-1-yl)malononitrile* (**21**) *to 2-(4,5-dihydroxy-2-methylphenyl)malononitrile* (**20**) and this the corresponding cathodic peak of (A_0). The influence of the CV scan rate on the reaction was also studied, according to a previous report [20], and the reactivity of these compounds was observed. The optimum condition for the pH was determined to be 7.2 according to the procedure explained elsewhere [21, 22].

For the electro-organic synthesis of *2-(4,5-dihydroxy-2-methylphenyl)malononitrile* (**20**) and *2-(6-methyl-3,4-dioxocyclohexa-1,5-dienyl)malononitrile* (**21**) (Scheme 3), 1 mmol of *4-methylcatechol* (**18**) and 1 mmol of *malononitrile* (**8**) were dissolved in 100 mL of the buffer solution Na_2HPO_4/NaH_2PO_4 (0.2 M, pH 7.2), and the solution was electrolyzed at 5 mA for 48 h in an undivided cell (by galvanostatic mode). During the electrolysis, the process was interrupted a few times, and the graphite anode was washed in acetone and polished in order to reactivate its surface. After the electrolysis step, the products were filtered and washed with water. The products were characterized using FT-IR, ^{1}H NMR, ^{13}C NMR, mass spectrometry (MS), and elemental analysis.

2-(4,5-Dihydroxy-2-methylphenyl)malononitrile (**20**) and *2-(6-methyl-3,4-dioxocyclohexa-1,5-dienyl)malononitrile* (**21**): IR (KBr) ν (cm^{-1}): 3191, 2926, 2211, 1649, 1485, 1263, 871. ^{1}H NMR (300 MHz, DMSO-d_6) δ (ppm): 1.96 (s, 3H, CH_3), 2.32 (s, 3H, CH_3), 6.71 (s, 1H, aromatic), 6.88 (s, 1H, aromatic), 7.26 (s, 1H, aromatic), 7.29 (s, 1H, aromatic), 8.51 (s, 2H, CH), 9.40 (s, 1H, OH), 9.49

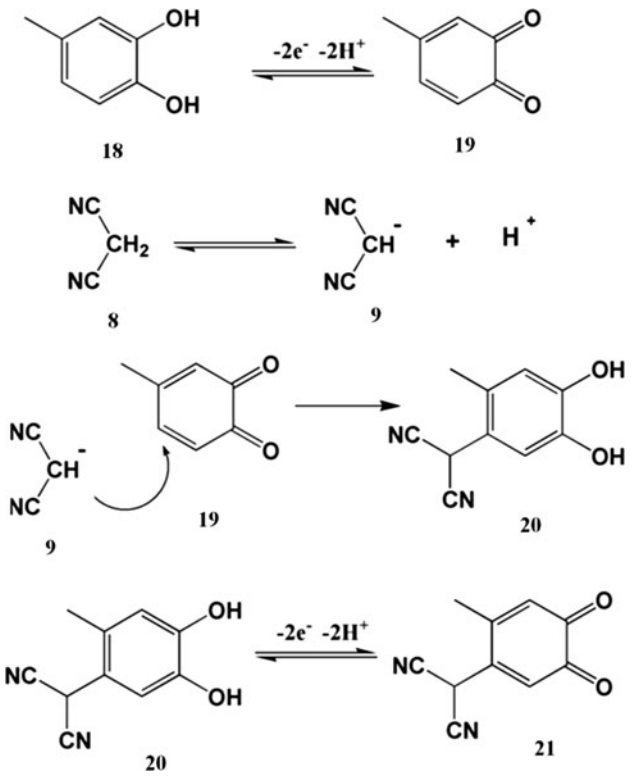

Scheme 3 Proposed mechanism for the electrooxidation of *4-methylcatechol* (**18**) in the presence of *malononitrile* (**8**)

(s, 1H, OH), ^{13}C NMR (75 MHz, DMSO-d_6) δ (ppm): 19.8, 20.5, 44.5, 60.4, 109.3, 115.0, 115.2, 115.6, 118.9, 120.5, 120.6, 122.2, 127.1, 130.8, 132.8, 144.5, 146.8, 147.4, 167.5. MS (EI, 70 eV) *m/z* (relative intensity): 188 (M^+ diol, 50), 186 (M^+ quinone, 40), 174 (M^+ quinone, 100), 172 (M^+ diol, 100), 155 (23), 124 (34), 89 (16), 44 (41), Anal. Calc. for $C_{20}H_{14}N_4O_4$: C, 64.17; H, 3.74; N, 14.97. Found: C, 64.23; H, 3.79; N, 15.03).

The proposed mechanism for the formation of *2-(4,5-dihydroxy-2-methylphenyl)malononitrile* (**20**) and *2-(6-methyl-3,4-dioxocyclohexa-1,5-dienyl)malononitrile* (**21**) is presented in Scheme 3.

3.2 Cyclic voltammetric studies of *chemically catechol-modified MCM-41* (**5**) with *malononitrile* (**8**)

To establish and prove the electrochemical reaction of *malononitrile* (**8**) with *chemically catechol-modified MCM-41* (**5**), 250 mg of *chemically catechol-modified MCM-41* (**5**) was suspended in the above-mentioned buffer solution, and its voltammogram was recorded (Fig. 1c, curve a). Based on the results obtained from the electrochemical activity of *4-methylcatechol* (**18**) and *malononitrile* (**8**) (Fig. 1a), it was concluded that the anodic peak A_1 and the corresponding cathodic peak C_1 were due to the transformation of *chemically catechol-modified MCM-41* (**5**) to *o-quinone-functionalized MCM-41* (**6**), and vice versa, within a quasireversible two-electron/two-proton reaction. Then, 250 mg of *chemically catechol-modified MCM-41* (**5**) and 25 mg of *malononitrile* (**8**) were added to the same buffer solution and studied by CV (Fig. 1c, curve b). As this CV shows, the cathodic peak (C_1) current decreased strongly. The observed decrease of this peak (C_1) in the cyclic voltammogram clearly indicates that *chemically catechol-modified MCM-41* (**5**) is electrochemically oxidized on the surface of the electrode, and is subsequently involved in a chemical reaction with *malononitrile* (**8**). Figure 1c, curve c is the voltammogram of solution containing 25 mg of *malononitrile* (**8**) in the same solution using the same conditions (Na_2HPO_4/NaH_2PO_4 (0.2 M, pH 7.2) buffer solution). The multicyclic voltammograms of the mixture containing *chemically catechol-modified MCM-41* (**5**) and *malononitrile* (**8**) were studied and as it was expected, in the second cycle, the voltammograms exhibit a relatively intense decrease in the anodic peak current A_1, along with some potential shift in the positive direction. The positive shift of the anodic peak in the second scan was due to the formation of a thin product film on the electrode surface, and this issue, to a certain extent, inhibits the performance of the electrode response [23–25].

3.3 Cyclic voltammetric studies of *catechol* (**12**) and *amine-functionalized MCM-41* (**3**)

In order to establish an electrochemical method for the functionalization of mesoporous silica, *catechol* (**12**) was dissolved in a buffer solution of Na_2HPO_4/NaH_2PO_4, and its voltammogram was recorded (2 mmol L^{-1}). The anodic peak A_1 and the corresponding cathodic peak C_1 shown in Fig. 1d, curve a are due to the transformation of *catechol* (**12**) to the corresponding *o-quinone* (**13**), and vice versa, via a quasireversible two-electron/two-proton reaction. During the reaction of *catechol* (**12**) to form *o-quinone* (**13**), the peak current ratio $I_p^{C_1}/I_p^{A_1}$ is nearly equal to 1.

The activity of 250 mg of *amine-functionalized MCM-41* (**3**) as a nucleophile in the presence of *catechol* (**12**) (2 mmol L^{-1}) was investigated using CV (Fig. 1d, curve b). In the reaction of *amine-functionalized MCM-41* (**3**) as a nucleophile with *o-quinone* (**13**), the cathodic peak current (C_1) decreased, due to the Michael reaction of *amine-functionalized MCM-41* (**3**) with *o-quinone* (**13**). To show that *amine-functionalized MCM-41* (**3**) does not have any cathodic or anodic peaks, its voltammogram was also recorded in the same solution and under the same conditions (Fig. 1d, curve c).

Table 1 MS data of compounds *malononitrile-functionalized MCM-41* (**10/11**) and *malononitrile-functionalized MCM-41* (**16/17**)

Mass	Relative intensity	Fragment formula	Suggested structure
200	56	$C_{10}H_6N_3O_2^{\bullet+}$	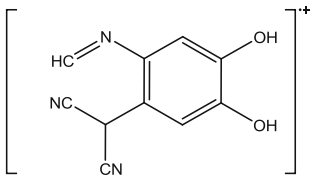
198	61	$C_{10}H_4N_3O_2^{\bullet+}$	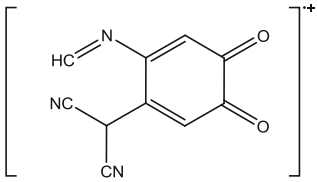
174	45	$C_9H_6N_2O_2^{\bullet+}$	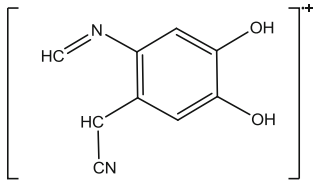
172	48	$C_9H_4N_2O_2^{\bullet+}$	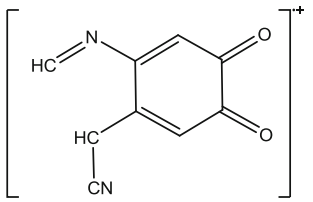
148	34	$C_8H_6NO_2^{\bullet+}$	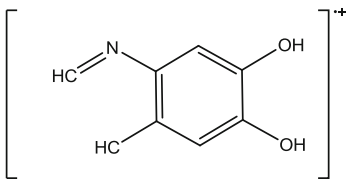
146	38	$C_8H_4NO_2^{\bullet+}$	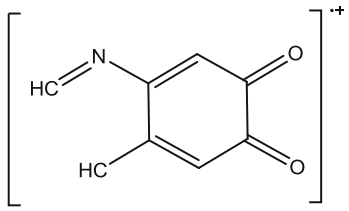
121	100	$C_7H_5O_2^{+}$	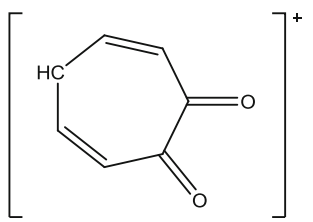

Table 1 continued

Mass	Relative intensity	Fragment formula	Suggested structure
91	83	$C_7H_7^+$	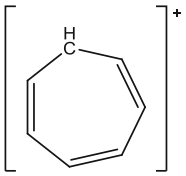
77	66	$C_6H_5^+$	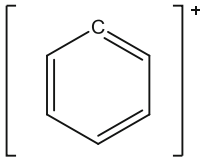
65	58	$C_3HN_2^+$	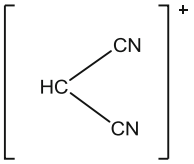

Fig. 2 The mass spectrum of **a** *malononitrile-functionalized MCM-41* (**10/11**); **b** *malononitrile-functionalized MCM-41* (**16/17**)

The multicyclic voltammograms of the mixture containing *amine-functionalized MCM-41* (**3**) and *catechol* (**13**) were studied, and the results are presented in Fig. 1e. In the second scan of the multicyclic voltammograms, a new anodic peak A_0 was also observed. This peak is related to the oxidation of the *electrochemically catechol-modified*

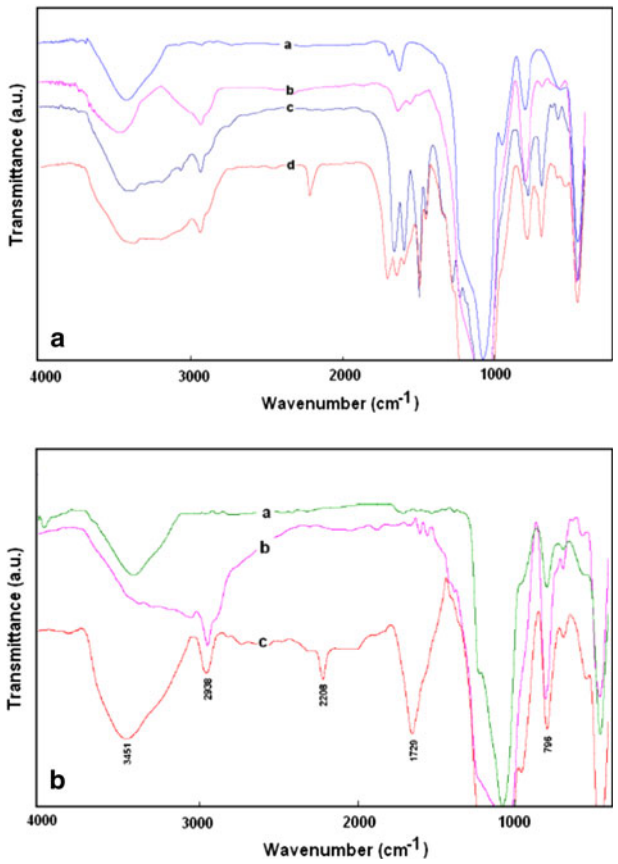

Fig. 3 Infared spectrum of **a** (*a*) *MCM-41* (**1**), (*b*) *amine-functionalized MCM-41* (**3**), (*c*) *chemically catechol-modified MCM-41* (**5**), (*d*) *malononitrile-functionalized MCM-41* (**10/11**); **b** (*a*) *MCM-41* (**1**), (*b*) *amine-functionalized MCM-41* (**3**), (*c*) *malononitrile-functionalized MCM-41* (**16/17**)

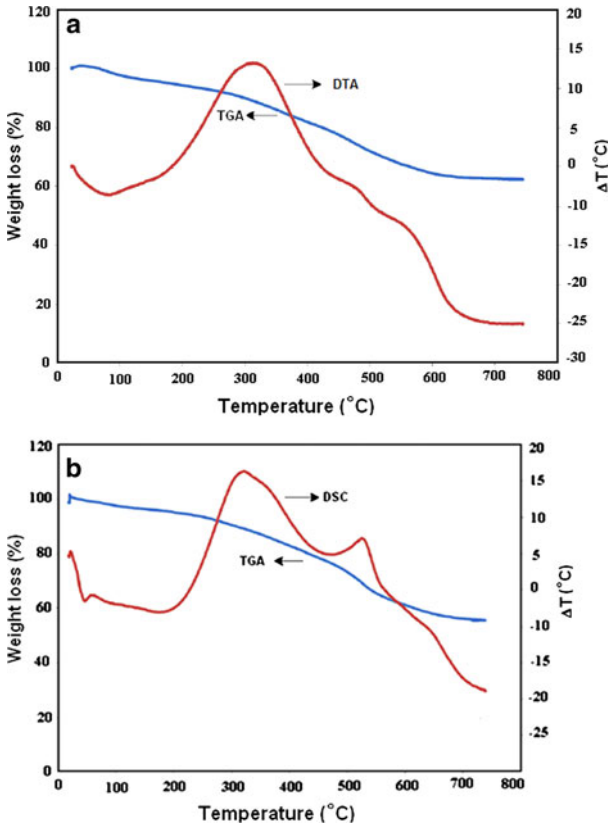

Fig. 4 TGA–DTA of **a** *malononitrile-functionalized MCM-41* (**10/11**); **b** *malononitrile-functionalized MCM-41* (**16/17**)

Table 2 IR data of compounds *MCM-41* (**1**), *amine-functionalized MCM-41* (**3**), *chemically catechol-functionalized MCM-41* (**5**), *malononitrile-functionalized MCM-41* (**10/11**), and *malononitrile-functionalized MCM-41* (**16/17**)

Group	IR wave number (cm^{-1})				
	(**1**)	(**3**)	(**5**)	(**10/11**)	(**16/17**)
NH & OH	3,000–3,500	3,000–3,500	3,000–3,500	3,000–3,500	3,000–3,500
CH aliphatic	–	2,941	2,945	2,943	2,938
CN	–	–	–	2,210	2,208
C=O	–	–	–	1,727	1,729
C=N	–	–	1,690	1,683	1,680
C=C	–	–	–	1,619	1,620
Si–O–Si	1,040	1,040	1,040	1,040	1,040
NH	–	799	800	801	796

MCM-41 (**14**) to *o-quinone-modified MCM-41* (**15**). By comparing the results of this section to the results of the section titled: *Study of the reactivity of catechol with malononitrile*, it can be concluded that catechol shows the same reactivity with both nucleophiles.

3.4 Characterization of *malononitrile-functionalized MCM-41* (**10/11**)

Malononitrile-functionalized MCM-41 (**10/11**) was characterized by IR and MS. The heat treatment of *malononitrile-*

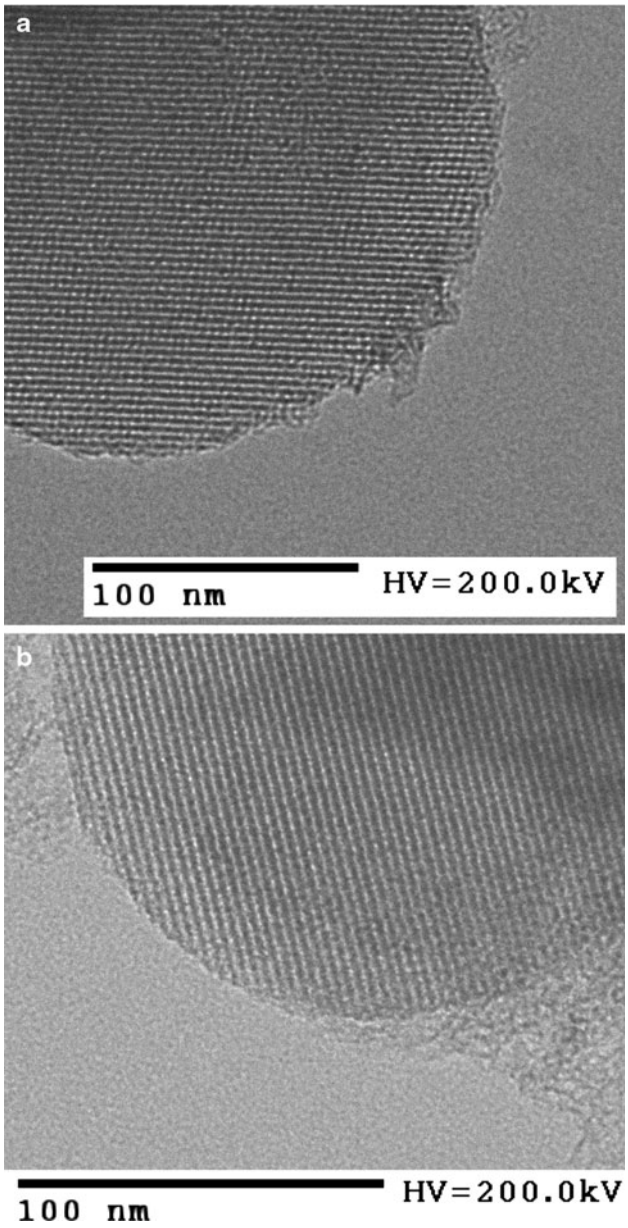

Fig. 5 The TEM micrograph of synthesized **a** *malononitrile-functionalized MCM-41* (**10/11**); **b** *malononitrile-functionalized MCM-41* (**16/17**)

functionalized MCM-41 (**10/11**) in the vacuum chamber of the mass spectrometer released organic species with *m/z* values of 200, 198, 174, 172, 148, 146, 121, 91, 77, and 65, which correspond to $C_{10}H_6N_3O_2^{\bullet+}$, $C_{10}H_4N_3O_2^{\bullet+}$, $C_9H_6N_2O_2^{\bullet+}$, $C_9H_4N_2O_2^{\bullet+}$, $C_8H_6NO_2^{\bullet+}$, $C_8H_4N_2^{\bullet+}O$, $C_7H_5O_2^{+}$, $C_7H_7^{+}$, $C_6H_5^{+}$, and $C_3HN_2^{+}$ fragments, respectively (Table 1). The mass spectrum of *malononitrile-functionalized MCM-41* (**10/11**) is presented in Fig. 2a. The suggested fragments in Table 1 are in a good agreement with the expected fragments of *malononitrile-functionalized MCM-41* (**10/11**) and unambiguously demonstrate its formation. The IR spectra of the synthesized materials in each step are shown in Fig. 3a, and peak assignments are listed in Table 2. As can be seen, the spectrum of *malononitrile-functionalized MCM-41* (**10/11**) shows new absorption bands in the range of 2,300–1,600 cm^{-1} in comparison with the spectrum of *amine-functionalized MCM-41* (**3**). The appearance of two distinct bands at 2,217 and 1,710 cm^{-1} as a result of the presence of CN and carbonyl groups unambiguously confirmed the formation of *malononitrile-functionalized MCM-41* (**10/11**). A similar low-angle XRD pattern of *MCM-41* (**1**) and *malononitrile-functionalized MCM-41* (**10/11**) confirmed that the mesoporous structure was maintained after functionalization. The density of the functional groups grafted onto the mesoporous silica was obtained by elemental and TGA–DTA (Fig. 4a). According to the elemental analysis, the amount of grafted organic modifiers was found to be 1.68 mmol g^{-1}. The TGA–DTA confirmed the elemental analysis data by showing a 38 % weight loss for the functionalized material in the TGA curve, which corresponds to 1.66 mmol g^{-1} grafted organic modifiers. The TEM micrograph shows the nanostructure remains after functionalization (Fig. 5a). Finally, the surface area of the composite after grafting the functional groups, which was measured by nitrogen sorption analysis (S_{BET}, 493 m^2 g^{-1}), showed that the high-surface area of the mesoporous silica was maintained after the electrochemical functionalization. The proposed mechanism for the formation of *malononitrile-functionalized MCM-41* (**10/11**) is shown in Scheme 1.

3.5 Characterization of *malononitrile-functionalized MCM-41* (**16/17**)

Malononitrile-functionalized MCM-41 (**16/17**) was analyzed by IR spectroscopy and MS. The heat treatment of *malononitrile-functionalized MCM-41* (**16/17**) in the vacuum chamber of the mass spectrometer released organic species with *m/z* values of 202, 200, 176, 174, 150, 148, 136, 134, 121, 91, 77, and 65, which correspond to $C_{10}H_8N_3O_2^{\bullet+}$, $C_{10}H_6N_3O_2^{\bullet+}$, $C_9H_8N_2O_2^{\bullet+}$, $C_9H_6N_2O_2^{\bullet+}$, $C_8H_8NO_2^{\bullet+}$, $C_8H_6NO_2^{\bullet+}$, $C_7H_6NO_2^{\bullet+}$, $C_7H_4NO_2^{\bullet+}$, $C_7H_5O_2^{+}$, $C_7H_7^{+}$, $C_6H_5^{+}$, and $C_3HN_2^{+}$ fragments, respectively (Table 3). The mass spectrum of *malononitrile-functionalized MCM-41* (**10/11**) is presented in Fig. 2b.The suggested fragments shown in Table 3 are in good agreement with the expected fragments from *malononitrile-functionalized MCM-41* (**16/17**). The IR spectra of the functionalized mesoporous silica in different steps have been compared in Fig. 3b, and peak assignments are listed in Table 2. As can be seen in Fig. 3b, *malononitrile-functionalized MCM-41* (**16/17**) shows new bands in the range of 2,300–1,600 cm^{-1} in comparison with the

Table 3 MS data of compounds *malononitrile-functionalized MCM-41* (**16/17**)

Mass	Relative intensity (%)	Fragment formula	Suggested structure
202	46	$C_{10}H_8N_3O_2^{\bullet+}$	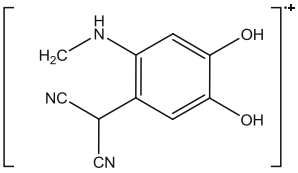
200	58	$C_{10}H_6N_3O_2^{\bullet+}$	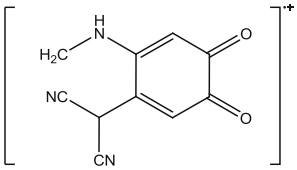
176	37	$C_9H_8N_2O_2^{\bullet+}$	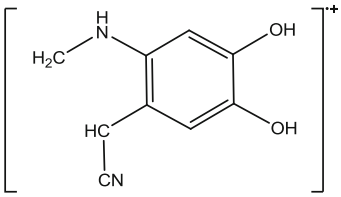
174	41	$C_9H_6N_2O_2^{\bullet+}$	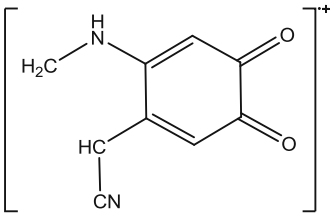
150	30	$C_8H_8NO_2^{\bullet+}$	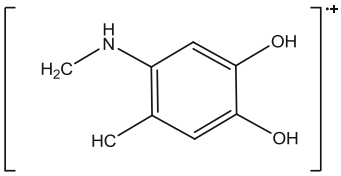
148	35	$C_8H_6NO_2^{\bullet+}$	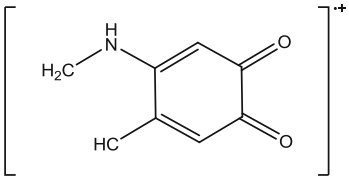
136	34	$C_7H_6NO_2^{\bullet+}$	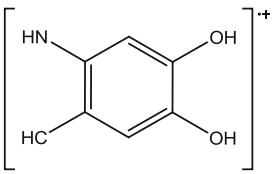
134	38	$C_7H_4NO_2^{\bullet+}$	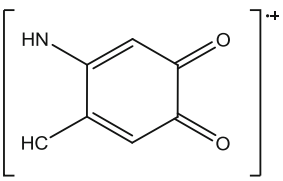

Table 3 continued

Mass	Relative intensity (%)	Fragment formula	Suggested structure
121	100	$C_7H_5O_2^+$	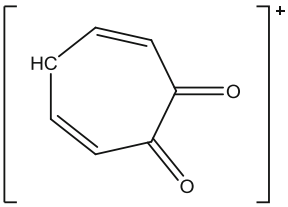
91	85	$C_7H_7^+$	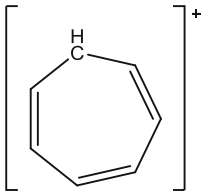
77	65	$C_6H_5^+$	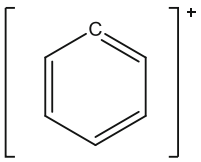
65	75	$C_3HN_2^+$	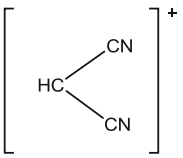

spectrum of *amine-functionalized MCM-41* (**3**). The appearance of these new bands at 2,208 and 1,729 cm^{-1} showed that the CN and carbonyl groups were incorporated in the final *malononitrile- functionalized MCM-41* (**16/17**) compound. The low-angle XRD pattern of *malononitrile-functionalized MCM-41* (**16/17**) also confirmed that the mesoporous structure was maintained after functionalization by the electrochemical method. The densities of the functional groups grafted onto the mesoporous silica were obtained by elemental and TGA–DTA (Fig. 4b). According to the elemental analysis, the amount of grafted organic modifiers was determined to be 1.85 mmol g^{-1}. The TGA–DTA confirmed the elemental analysis data showing a 43 % weight loss for the functionalized material in the TGA curve, which corresponds to 1.87 mmol g^{-1} grafted organic modifiers. The TEM micrograph shows the nanostructure remains after functionalization (Fig. 5b). Finally, the surface area measurement of MCM-41 after grafting the functional groups (S_{BET}, 451 m^2 g^{-1}) showed that the high-surface area of the mesoporous silica was maintained. The proposed mechanism for the formation of *malononitrile-functionalized MCM-41* (**16/17**) is shown in Scheme 2.

3.6 Application of *malononitrile-functionalized MCM-41* (**16/17**) as an Au(III) sorbent

As an application, *malononitrile-functionalized MCM-41* (**16/17**) was used for the separation and preconcentration of gold from an aqueous solution. All studies were performed according to previous report on adsorption of gold on mesoporous silica materials [26].

Considering the important role of pH on solid phase extraction, the optimum conditions for the pH were obtained by placing 10 mg of sorbent in 50 mL of different sample solutions containing 1 mg L^{-1} gold ion with pH in the range of 1–8. Then the sorbent was washed with 10 mL of thiourea 1 mol L^{-1} in 3 mol L^{-1} H_2SO_4 and the eluent was analyzed with FAAS. The optimum extraction condition was obtained at pH of 2 (Fig. 6).

The selectivity of the sorbent for gold extraction in the presence of different cations was also studied. The cations of Na^+, K^+, Cs^+, Mg^{2+}, Ca^{2+}, Cd^{2+}, Cs^+, Fe^{2+}, Cu^{2+}, Pb^{2+}, and Cr^{3+} as their chloride salts with various concentrations were added to 100 mL of single solution containing 1 mg of gold and the extraction procedure was followed. The tolerable amount was defined as the

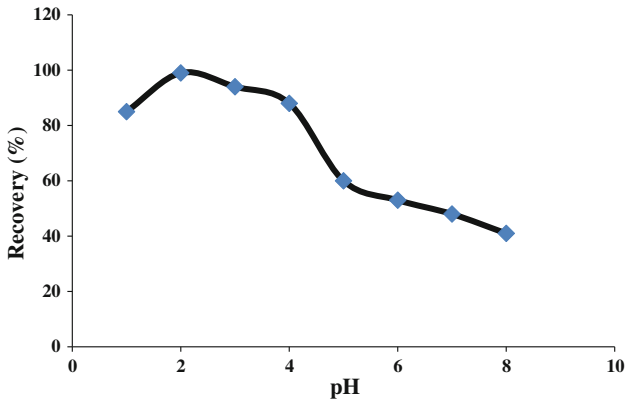

Fig. 6 Effect of pH on recovery of gold ions on *malononitrile-functionalized MCM-41* (**16/17**)

Table 4 The tolerance limit of the diverse ions on the determination of gold

Interfering ions	Tolerable concentration	R ± RSD %
Na^{+}	2,500	98.8 ± 1.1
K+	2,500	98.9 ± 1.2
Cs+	2,500	99.1 ± 1.1
Ca^{2+}	2,500	98.8 ± 1.3
Mg^{2+}	2,500	98.9 ± 0.9
Cd^{2+}	1,000	98.7 ± 1.0
Pb^{2+}	1,000	96.1 ± 1.3
Cu^{2+}	500	97.2 ± 1.5
Cr^{3+}	500	97.4 ± 1.5
Fe^{2+}	500	96.8 ± 1.6

maximum concentration which could cause a change of less than 5 % in signal compared to the signal of each ion without any interference. The results showed that the presence of these cations has no effect on the recovery of gold ions and the sorbent is selective toward gold ions in pH = 2.0 (Table 4).

The maximum adsorption capacity of *malononitrile-functionalized MCM-41* (**16/17**) for gold ions was studied by placing 10 mg of *malononitrile-functionalized MCM-41* (**16/17**) in 500 mL portions of aqueous single solutions containing 5 mg gold. After adjusting pH and extracting, the gold ions were determined by their amount in eluent using FAAS. The maximum capacity was found to be 329 ± 6 mg g^{-1}.

The precision of the method under the optimal conditions was determined by performing ten replicates. The gold recovery was found to be 99.1 ± 1.2 %.

4 Conclusions

Modification of mesoporous silica is essential to achieve new applications of these materials. Conventional methods for medication of these materials are limited and usually require application of catalysts, solvents and heating. In this paper, malononitrile-functionalized mesoporous silica was synthesized using an electrochemical method and characterized by electrochemical and spectroscopic techniques. The application of the synthesized material for Au(III) adsorption was investigated. The results of this work show that electrochemical modification of mesoporous silica can be used as a new green novel tool for grafting functional groups onto these materials in the room temperature. The presented method can result in the appearance of new applications of mesoporous materials.

Acknowledgments The authors wish to thank the Vice-President's office for Research Affairs of Shahid Beheshti University for supporting this work.

References

1. Pang J, Hampsey JE, Hu Q, Wu Zh, John VT, Lu Y (2004) Mesoporous silica with Ia3d cubic structure and good thermal stability. Chem Commun 40:682
2. Lu AH, Nitz J, Comotti M, Weidenthaler C, Schlichte K, Lehmann CW, Terasaki Os, Schuth F (2010) Spatially and size selective synthesis of Fe-based nanoparticles on ordered mesoporous supports as highly active and stable catalysts for ammonia decomposition. J Am Chem Soc 132:14152
3. Sayari A, Belmabkhout Y (2010) Stability of amine-containing CO_2 adsorbents. J Am Chem Soc 132:6312
4. Davis ME (2002) Ordered porous materials for emerging applications. Nature 417:813
5. Farrell RA, Cherkaoui K, Petkov N, Amenitsch H, Holmes JD, Hurley PK, Morris MA (2007) Physical and electrical properties of low dielectric constant self-assembled mesoporous silica thin films. Microelectron Reliab 47:759
6. Qi H, Shopsowitz KE, Hamad WY, MacLachlan MJ (2011) Chiral nematic assemblies of silver nanoparticles in mesoporous silica thin films. J Am Chem Soc 133:3728
7. Haitao Yu, Pengcheng Xu, Xiaoyuan Xia, Lee D-W, Xinxin Li (2012) Micro/nano-combined gas sensors with functionalized mesoporous thin-film self-assembled in batches onto resonant cantilevers. IEEE Trans. Ind. Electron. 59:4881
8. Pengcheng Xu, Haitao Yu, Xinxin Li (2011) Functionalized mesoporous silica for microgravimetric sensing of trace chemical vapors. Anal Chem 83:3448
9. Knezevic NZ, Trewyn BG, Lin VSY (2011) Functionalized mesoporous silica nanoparticle-based visible light responsive controlled release delivery system. Chem Comm 47:2817
10. Anwander R, Nagl I, Widenmeyer M, Engelhardt G, Groeger O, Palm C, Roser T (2000) Surface characterization and derivatization of MCM-41 silicas via silazane silylation. J Phys Chem B 104:3532
11. Yamamoto K, Tatsumi T (2001) Organic functionalization of mesoporous molecular sieves with Grignard reagents. Microporous Mesoporous Mater 44:459
12. Bruhwiler D (2010) Postsynthetic functionalization of mesoporous silica. Nanoscale 2:887
13. Maleki A, Nematollahi D (2009) An efficient electrochemical method for the synthesis of methylene blue. Electrochem Commun 11:2261
14. Nematollahi D, Rafiee M (2005) Diversity in electrochemical oxidation of dihydroxybenzoic acids in the presence of

acetylacetone. A green method for synthesis of new benzofuran derivatives. Green Chem 7:638
15. Nematollahi D, Afkhami A, Tammari E, Shariatmanesh T, Hesari M, Shojaeifard M (2007) An efficient electrochemical synthesis of diamino-o-benzoquinone: mechanistic and kinetic evaluation of the reaction of azide ion with o-benzoquinone. Chem Commun 43:162
16. Schumacher K, Grün M, Unger KK (1999) Novel synthesis of spherical MCM-48. Microporous Mesoporous Mater 27:201
17. Johnson BJS, Stein A (2001) Surface modification of mesoporous, macroporous, and amorphous silica with catalytically active polyoxometalate clusters. Inorg Chem 40:801
18. Papouchado L, Petrie G, Adams RNJ (1972) Anodic oxidation pathways of phenolic compounds: Part I. Anodic hydroxylation reactions. J Electroanal Chem 38:389
19. Nematollahi D, Rafiee M, Samadi-Maybodi A (2004) Mechanistic study of electrochemical oxidation of 4-tert-butylcatechol: a facile electrochemical method for the synthesis of new trimer of 4-tert-butylcatechol. Electrochim Acta 49:2495
20. Hosseiny Davarani SS, Sheijooni Fumani N, Arvin-Nezhad H, Moradi F (2008) Electrochemical synthesis of 6-amino-5-(3,4-dihydroxyphenyl) pyrimidine. Tetrahedron Let 49:710
21. Nematollahi D, Rafiee M (2006) Electrochemical oxidation of catechols in the presence of acetylacetone. J Electroanal Chem 566:31
22. Rafiee M, Nematollahi D (2009) Electrochemical oxidation of catechols in the presence of cyanoacetone and methyl cyanoacetate. J Electroanal Chem 626:36
23. Hosseiny Davarani SS, Fakhari AR, Shaabani A, Ahmar H, Maleki A, Sheijooni Fumani N (2008) A facile electrochemical method for the synthesis of phenazine derivatives via an ECECC pathway. Tetrahedron Lett 49:5622
24. Bayandori Moghaddam A, Kobarfard F, Fakhari AR, Nematollahi D, Hosseiny Davarani SS (2005) Electrochim Acta 51:739
25. Hosseiny Davarani SS, Fakhari AR, Sheijooni Fumani N, Kalatebojdi M (2008) Electrochemical synthesis of new benzodifurans. Electrochem Commun 10:1765
26. Ebrahimzadeh H, Tavassoli N, Sadeghi O, Amini MM, Jamali M (2011) Comparison of novel pyridine-functionalized mesoporous silicas for Au(III) extraction from natural samples. Microchim Acta 172:479